

# Design, modelling and testing of a compact piezoelectric transducer for railway track vibration energy harvesting

Guansong Shan, Yang Kuang, Meiling Zhu \*

College of Engineering, Mathematics and Physical Sciences, University of Exeter, Exeter, UK

## ARTICLE INFO

### Keywords:

Vibration energy harvesting  
Piezo stack  
Mechanical transformer  
Frequency up-conversion  
Railway track

## ABSTRACT

To enable wireless sensor networks to monitor rail infrastructures in real-time, a cost-effective power source is in need. This work presents the design, modelling and testing of a piezo stack energy harvester with frequency up-conversion mechanism for scavenging energy from railway track vibration. The proposed harvester is designed to meet railway track applications' size, frequency, and stress requirements. A compact design integrating the inertial mass and the piezo stack transducer systems is used to enable the mechanical collision for realising the frequency up-conversion mechanism and ensure the size of the energy harvester is suitable for the limited space on the railway track. The frequency bandwidth of the energy harvester is broadened by utilizing the longitudinal and torsional oscillation of the designed plate springs which enable the system to have two adjacent natural frequencies. The mechanical transformer of the piezo stack transducer system is designed to achieve the required stress level under both the impact force caused by the collision motion and the inertial force generated by the random vibration of the rails. A finite element model (FEM) analysing the free vibration of the piezo stack transducer caused by the frequency up-conversion mechanism is developed to analyse the dynamic characteristics of the coupled system. Lab tests are carried out to validate the proposed FEM and evaluate the impact of different factors such as load resistance, acceleration, initial interval, plate spring, and pulse excitation on power generation. Experimental results show that the energy harvester has two resonant frequencies of 17 Hz and 20 Hz. The frequency up-conversion mechanism can convert this low-frequency vibration into the piezo stack transducer's high resonant frequency vibration of 94 Hz. A maximum average power of 6.72 mW with a 1-mW-bandwidth of 15 Hz is obtained when actuated at 0.7 RMS g acceleration.

## 1. Introduction

Rail transportation systems are essential to society. More than 4 million rolling stock per year globally uses around 854,000 kilometres of railway lines [1]. To monitor railway line infrastructures in real-time and detect faults before they cause any damage, condition monitoring based on wireless sensor networks (WSNs) has attracted significant attention due to their excellent flexibility and low installation cost. However, one major challenge with WSNs is the power source. Conventional batteries have a limited lifetime. Replacing or recharging batteries can be difficult when the sensor nodes are distributed in a large area and large number. In this regard, energy harvesting provides a promising solution by converting the ambient energy sources to supply the WSNs.

There is a vast energy potential for harvesting from the railway track vibration [2]. Aiming at transforming the mechanical energy into

electrical energy, researchers have studied different energy harvesting technologies, such as electromagnetic and piezoelectric. For example, Gao et al. [3] designed a linear harvester with a spring, magnet and coil according to the limited space of the railway track utilising the relative translational motion of the coil and magnet to achieve a peak power of 119 mW. Pan et al. [4] designed a ball screw based harvester using the combination of speed-increasing drivetrains and rotary electromagnetic generators, and an average power of 1.12 W was obtained in field tests with the harvester clamped on the railway track. However, a moving magnet is hard to be implemented in a metallic environment for translational electromagnetic harvesters [5]. At the same time, the mechanical efficiency is typically low [6] and the volume is relatively sizeable impeding track regular maintenance [7] for rotary electromagnetic harvesters.

Besides electromagnetic harvesters, piezoelectric energy harvesters have been investigated recently due to their high energy and power

\* Corresponding author.

E-mail address: [m.zhu@exeter.ac.uk](mailto:m.zhu@exeter.ac.uk) (M. Zhu).

density, simple structure, good scalability, ease of application and versatile shapes [8–10]. Gao et al. [11] used a cantilever with PZT film attached to it for railway track application, and a peak power of 4.9 mW was achieved in lab tests when actuated at 5 g and 7 Hz, however the power level is low and cantilevers possess high fracture risk since the acceleration of the railway track vibration is quite high [12]. Simply supported beams [12] were proposed to tackle the fracture problem of the cantilever. Lab tests showed that a single simply supported beam can generate 380  $\mu$ W at resonance with the optimal load resistor of 20 k $\Omega$ . Apart from the linear piezoelectric energy harvesters, nonlinearity has been introduced into piezoelectric railway energy harvesting system recently to widen the frequency bandwidth. A harvester composed of a hosting beam and a group of micro-beams with repulsive magnetic forces on their free ends [13] was proposed to broaden the harvesting bandwidth and achieved a maximum RMS power of 16  $\mu$ W in lab tests. Although most research focuses on bending modes of piezoelectric materials for railway energy harvesting, compression modes have also been investigated due to their higher coupling factor. Cao et al. [14] proposed a piezo stack device utilising the compression mode of piezoelectric materials and achieved a maximum average power of 0.34 mW. In order to increase the average power level of piezoelectric energy harvesters for railway track vibration from  $\mu$ W to mW, the idea of combining a piezo stack with compression mode, a mechanical transformer and frequency up-conversion mechanism for railway tracks was proposed in our previous work [15], but several requirements of track vibration were not considered. First, there is limited space for installing the energy harvester on the railway track without impeding track maintenance like tamping. Second, the strength of the energy harvester should satisfy the high acceleration of the railway track vibration. Third, the frequency bandwidth needs to be broadened to improve the energy harvesting performance. As a result, a compact piezoelectric energy harvester which meets the requirements of railway track environment including size, stress, frequency is needed while maintaining the average power level of mW.

In this paper, a compact piezo stack energy harvester design with frequency up-conversion mechanism is proposed for scavenging energy from railway track vibration. It consists of two systems integrated into one design: the inertial mass and the piezo stack transducer systems. The frequency bandwidth of the energy harvester is broadened by using two adjacent natural frequencies caused by the first and second mode of vibration of the inertial mass system. This is achieved through the longitudinal and torsional oscillation of the designed plate springs. The mechanical transformer is designed to achieve the required stress level under both the impact force caused by the collision motion and the inertial force generated by the random vibration of the rails. A FEM model considering the impact between the inertial mass system and the piezo stack transducer system is developed to analyse the dynamic characteristics. Lab tests are carried out to examine the performance of the harvester and validate the model. Experimental results show that the energy harvester has two resonant frequencies of 17 Hz and 20 Hz, and a maximum average power of 6.72 mW with a 1-mW-bandwidth of 15 Hz is obtained when actuated at 0.7 RMS g acceleration.

This paper is organised as follows. Section 2 introduces the detailed design and working principle of the proposed piezo stack energy harvester. Section 3 illustrates the system dynamics and finite element methods for modelling the proposed energy harvester. Section 4 is the fabrication and lab tests, and Section 5 is the results and discussions of simulation and experiments. Section 6 provides the concluding remarks.

## 2. Design of the energy harvester

### 2.1. Design considerations

#### 2.1.1. Installation

The typical ballasted track structure consists of railway tracks, railway pads, sleepers, the ballast and the subgrade [16]. It is reported that

the average vibration energy level decreases from railway tracks to subgrade due to the energy stored and consumed in each part [17]. As a result, this paper uses the railway tracks' vibration as the vibration source to design the energy harvester. Fig. 1 shows a photo of the implemented energy harvester installed on the railway track using two rail clamps.

#### 2.1.2. Size

The size of the harvester is restricted due to the installation requirement. The space available for the harvester on the railway track is approximately  $470 \times 100 \times 90 \text{ mm}^3$  according to spacings between sleepers and maintenance regulations [18]. Therefore, the proposed harvester is designed to be  $\Phi 90 \times 82 \text{ mm}^3$ .

#### 2.1.3. Resonant frequency and excitation

It is reported that in the frequency range below 30 Hz, the railway track vibration is predominantly due to the quasi-static moving axle load independent of the vehicle and track dynamics, and this frequency range is used for harvesting energy from railway track vibration [19,20]. Therefore, this frequency range is of interest in this paper. Fig. 2 shows an example of Fast Fourier Transform (FFT) result of railway track vibration, measured by the University of Birmingham in the time domain, and analysed by Energy Harvesting Research Group at the University of Exeter in the frequency domain when a wagon travelled at a maximum speed of 32 km/h tested in Long Marston, United Kingdom. The acceleration is relatively large below 5 Hz. It is challenging to design the harvester at such a low frequency, and such large acceleration may damage the harvester. Meanwhile, the second highest value occur between 16 and 21 Hz with acceleration amplitudes of approximately 1–2 g (RMS acceleration of 0.7–1.4 g when considered as harmonic excitation). As a result, we aim at the frequency range between 16 and 21 Hz as the target natural frequency of the energy harvester.

### 2.2. Design overview

Fig. 3 shows the schematic of the proposed energy harvester design based on the frequency up-conversion mechanism. It consists of two systems integrated into one design: the inertial mass system for adjusting the resonant frequency and the piezo stack transducer system for generating power. The inertial mass system comprises an inertial mass, two plate springs, and a structure for impacting with the piezo stack transducer system. The resonant frequency of the inertial mass system is designed to be around the dominant frequencies of the railway track vibration (16–21 Hz) by adjusting the inertial mass and plate springs. The piezo stack transducer system is constituted of a mechanical transformer, a multi-layer piezo stack polarised along the longitudinal direction ( $d_{33}$  mode), two plate springs and an added mass on the top. The mechanical transformer amplifies the vertical motion of the transformer into the axial movement of the piezo stack. The added mass reduces the resonant frequency of the piezo stack transducer and enhances

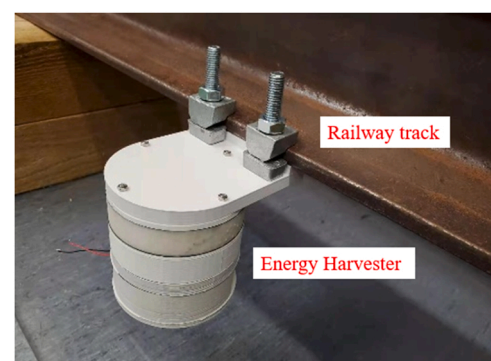


Fig. 1. A photo of the implemented energy harvester installed on the rail.

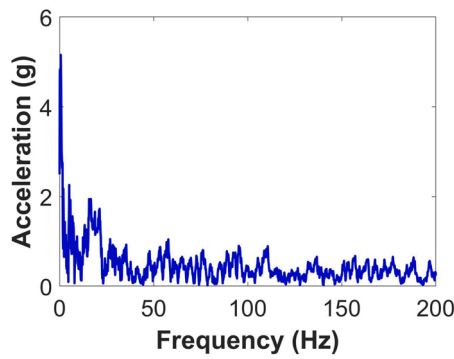


Fig. 2. An example of Fast Fourier Transform (FFT) result of railway track vibration when a wagon travelled at a maximum speed of 32 km/h tested in Long Marston, United Kingdom.

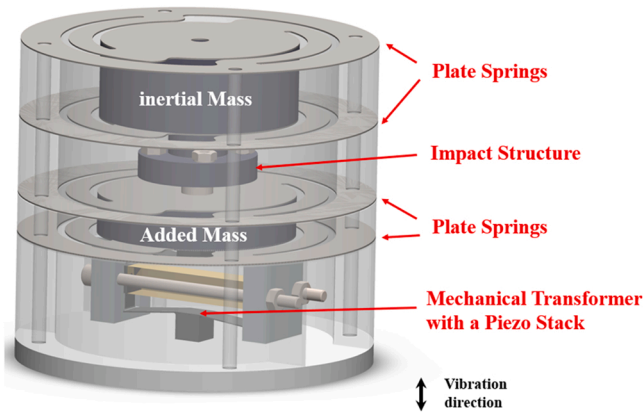


Fig. 3. A schematic of the proposed energy harvester design based on the frequency up-conversion mechanism.

its powering ability. The piezo stack converts the mechanical energy into electrical power when connected to an external load.

2.3. Working principle

Fig. 4 shows the output voltage of the proposed energy harvester illustrating the working principle. When there is vibration in the railway tracks, the inertial mass system oscillates at a resonant state and starts to approach the piezo stack transducer system at the first step. As the inertial mass system contacts and collides with the piezo stack transducer system in the second step, a large impact force is exerted and the voltage

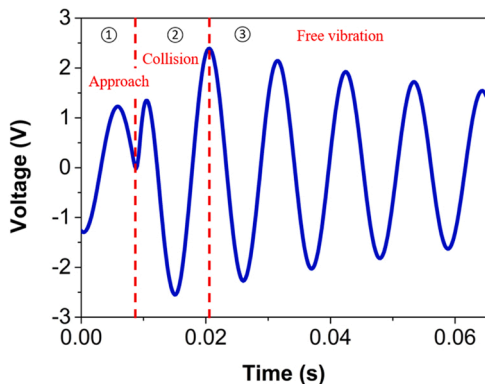


Fig. 4. The output voltage of the proposed energy harvester illustrating the working principle.

reaches maximum. As the inertial mass system travels upwards and away from the piezo stack transducer system, the two systems are separated, leading to free vibration of the piezo stack transducer system at its resonance frequency in the third step. This free vibration continues until the subsequent collision occurs. In this way, the energy harvester converts the low-frequency railway track vibration into the piezo stack transducer’s high resonant frequency oscillation. Without the frequency up-conversion mechanism, the piezo stack transducer would operate in the off-resonant mode under low-frequency excitations due to its high stiffness, thereby having a low power output. It is reported that the typical piezo stack transducer with a resonant frequency of 243 Hz worked in off-resonant mode at 3 Hz excitation, and only produced a maximum power of 0.0224 μW [21]. Therefore, the frequency up-conversion mechanism is crucial to the high-power generation of the energy harvester.

2.4. Design of the mechanical transformer

Stress analysis is essential to ensure the reliability of the harvester. The mechanical transformer is the weakest part of the energy harvester and can be damaged by the impact between the inertial mass system and the piezo stack transducer system if not designed properly. In this work, a model of the piezo stack transducer system is developed in Solidworks to help analyse the maximum stress and redesign the transformer, as shown in Fig. 5. The model includes both transformer and piezo stack with contact interaction. One end of the mechanical transformer is fixed while the other is applied with a mass of 0.15 kg. The transformer material is spring steel of 60Si2CrVA, which has a yield strength of about 1645 MPa and a fatigue strength of about 750 MPa [22]. The mechanical damping of the transducer is specified with a mechanical quality factor  $Q_M = 60$  of the piezo stack.

The mechanical transformer withstands two kinds of forces in railway applications. One is the impact force caused by the collision motion between the inertial mass system and the piezo stack transducer system. The other one is the inertial force generated by the random vibration of the railway tracks. The two forces are analysed by separate studies under Linear Dynamic Study respectively.

(1) Impact force caused by the collision motion

The impact force can be modelled as a triangular function [23]. Thus, Modal Time History analysis is used and a force with a defined triangular function is applied to the centre of the upper transformer. According to the measured velocity and impact force formula [15], the impact time and a peak triangular impact force function of 100 N are determined and used in the model. The impact force not only affects the maximum stress on the mechanical transformer, but also influences the input work of the mechanical transformer. The maximum input work of the mechanical transformer  $W$  is defined as the following equation:

$$W = F_{in}x_{in} \tag{1}$$

where  $F_{in}$  is the input peak impact force and  $x_{in}$  is the corresponding

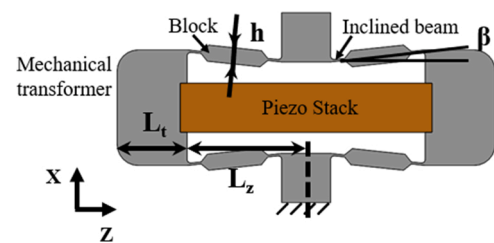


Fig. 5. The model and parameters for designing the mechanical transformer (the length of the transformer  $L_z$ , the thickness of the transformer  $L_t$ , the angle of the inclined beam  $\beta$  and the thickness of the block  $h$ ).

input displacement of the mechanical transformer. Fig. 6 shows the maximum stress and input work of the mechanical transformer with different input impact forces  $F_{in}$ . It is noted that a larger impact force will lead to higher input work and higher maximum stress. The more input work the mechanical transformer can get, the larger output work the piezo stack can generate, contributing to higher power output. However, if the maximum stress is larger than the yield and fatigue limit of the material, the mechanical transformer will break.

## (2) Inertial force generated by the random vibration of the railway tracks

The inertial force is modelled as a uniform base excitation and Random Vibration analysis is used. In the uniform base excitation, the PSD (power spectral density) curve accessed by transforming the time domain data of railway track vibration is input as the acceleration. The RMS responses are obtained as the simulation output and show the “one-sigma” root mean square values in terms of stress. Then we multiply those RMS values by three to meet the “three-sigma” criterion commonly used for fatigue evaluation. It means these stress levels will occur 99.7% of the time and it is considered safe when the stress limits are above those stress levels.

The maximum stress under impact force and random vibration with different parameters (the length of the transformer  $L_z$ , the thickness of the transformer  $L_t$ , the angle of the inclined beam  $\beta$  and the thickness of the block  $h$ ) are shown in Fig. 7. When  $h = 0.3$  mm, the thickness of the block is the same as that of the inclined beam. To achieve a lower maximum stress under both impact and random excitations, the mechanical transformer with  $L_z = 20$  mm,  $L_t = 3$  mm,  $\beta = 6^\circ$ ,  $h = 0.3$  mm is selected as shown in Fig. 8. The combined maximum stress under both excitations of the proposed transformer is 583 MPa, lower than the yield and fatigue limit of the material (1645 MPa and 750 MPa respectively), demonstrating the reliability of the harvester. In addition, the combined maximum stress of the proposed transformer is lower than that of our previous design [15] (745 MPa), and thus the proposed transformer has a superior strength.

## 2.5. Design of the plate springs

Two identical plate springs are used in the inertial mass system to adjust the resonant frequencies and guide the motion of the inertial mass, as shown in Fig. 9. Another pair of plate springs are added to the piezo stack transducer system to guide the motion of the added mass and prevent large torsion and damage of the mechanical transformer.

## 3. Finite element modelling

Finite element models are developed in COMSOL Multiphysics® to

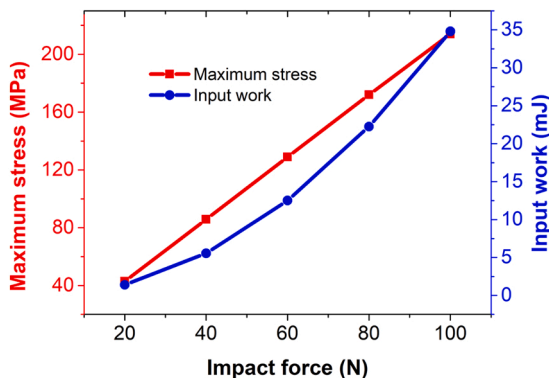


Fig. 6. The maximum stress and input work of the mechanical transformer with different input impact forces.

analyse the dynamic characteristics of the energy harvester. The previous models of longitudinal-mode piezoelectric energy harvesters mainly focus on their resonant responses under harmonic excitation [24–26]. The FEM developed in this work analyses the free vibration of the piezo stack transducer caused by the impact between the inertial mass system and the piezo stack transducer system.

The developed FEM model consists of two steps. Step (1), displacement simulation, is a time-dependent analysis which computes the displacements of the piezo stack transducer system under the impact motion between the inertial mass system and the piezo stack transducer system. Step (2), power generation simulation, is a time-dependent analysis that computes the voltage and power of the piezo stack using the calculated displacements in Step (1) as initial displacements.

### (1) Displacement simulation

In this step, the 3D physical model consists of two parts (inertial mass system and piezo stack transducer system) geometrically separated in the initial configuration forming a union with a contact pair. Only solid mechanics physics is used in this step. In the inertial mass system, a physical plate spring is used to analyse the resonant responses of the inertial mass system accurately. An added mass node of 0.3 kg is added to the top surface of the plate spring to simulate the inertial mass. A hemisphere is added to the bottom of the plate spring to make the collision a point-to-surface contact problem, which is easy to calculate for Comsol. The surface of the hemisphere is selected as the destination boundaries of the contact pair, while the top surface of the mechanical transformer of the piezo stack transducer system is chosen as the source boundaries of the contact pair, because the convex boundary should be the destination. In the piezo stack transducer system, the physical model consists of the mechanical transformer and the piezo stack. Two layers are added to the top of the mechanical transformer to apply the added mass node of 0.15 kg and the spring foundation node of 964 N/m, which simulate the added mass and plate springs in the piezo stack transducer system. The mechanical damping of the transducer is specified as a mechanical quality factor  $Q_M = 60$ . Fixed constraints are added to the bottom of the mechanical transformer and the edge of the plate spring. The penalty method is used in the contact boundary. Harmonic excitation of different frequencies is added as body load to the inertial mass system. A time-dependent analysis is used, and a parametric sweep of the excitation frequencies is performed. As a result, the maximum displacements of the top of the piezo stack transducer system are obtained across the frequency range of interest and input as initial displacements in Step (2).

### (2) Power generation simulation

In this step, the 3D physical model only consists of the piezo stack transducer system, of which the boundary conditions are the same as those in Step (1). The calculated displacements in Step (1) are used as initial displacements of the top of the mechanical transformer. Electrostatics and Electrical circuit physics are used to calculate the electrical output. The electrodes of the piezo stack are connected to a circuit with a load resistor. To simplify the model and reduce the computational time, we model the multilayer piezo stack as a single-layer piezoelectric element with the exact overall dimensions. Although power output and resonance frequency are not affected by the number of layers, values like impedance magnitude and voltage are different. The values of the single-layer piezoelectric element can be converted to those of the multilayer piezo stack using the following equations [26]:

$$\Gamma = \frac{\Gamma_s}{N^2} \quad (2)$$

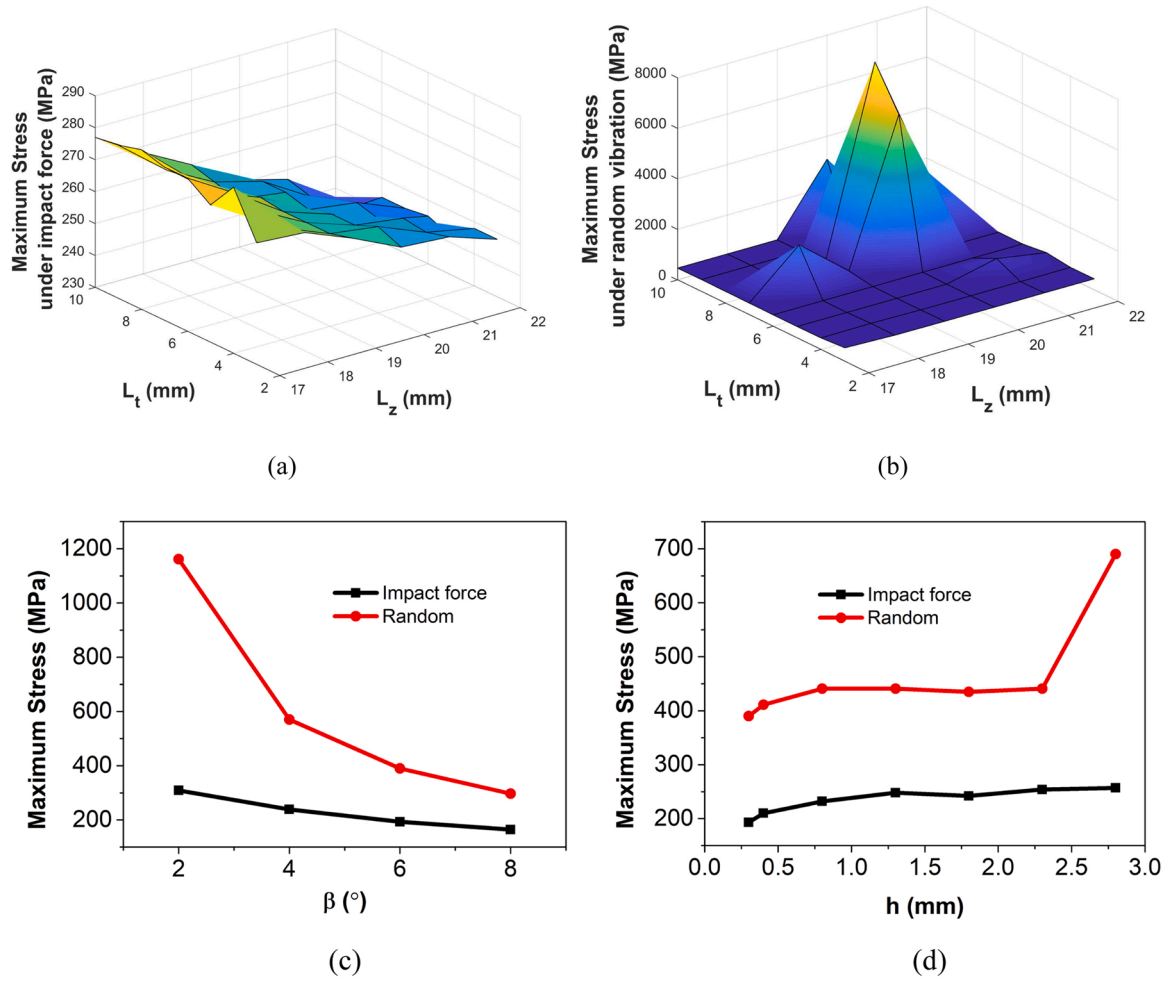


Fig. 7. The maximum stress under impact force and random vibration with different parameters: (a) length of the transformer  $L_z$ , (b) thickness of the transformer  $L_t$ , (c) angle of the inclined beam  $\beta$ , and (d) thickness of the block  $h$ .

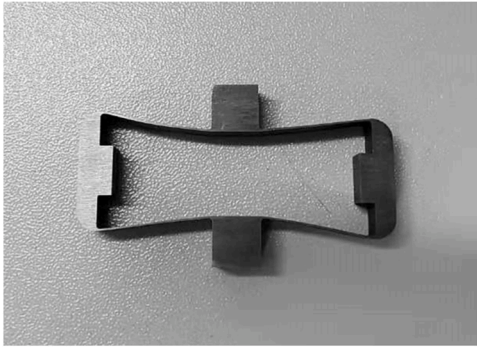


Fig. 8. The designed mechanical transformer with  $L_z = 20$  mm,  $L_t = 3$  mm,  $\beta = 6^\circ$ , and  $h = 0.3$  mm.

$$V = \frac{V_s}{N} \quad (3)$$

where  $\Gamma_s$  and  $V_s$  denote the impedance magnitude and the output voltage for single-layer piezoelectric element,  $\Gamma$  and  $V$  stand for the impedance magnitude and the output voltage for multilayer piezo stack respectively,  $N = 560$  is the number of piezoelectric layers. A time-dependent analysis is used for calculating responses for one cycle and a parametric sweep of the excitation frequency is performed. As a result, we can obtain the voltage

output and calculate the power output according to Eqs. (4, 5).

$$P = \frac{V^2}{R_L} \quad (4)$$

$$P_{ave} = \frac{V_{rms}^2}{R_L} \quad (5)$$

where  $V$  is the voltage output,  $P$  is the power output,  $R_L$  is the load resistance,  $P_{ave}$  is the average power output, and  $V_{rms}$  is the RMS voltage output.

## 4. Fabrication and lab tests

### 4.1. Fabrication

A prototype generator is fabricated based on the proposed design to test the energy harvesting performance. The inertial mass system consists of a 0.3 kg cylindrical inertial mass, two plate springs made of spring steel (0.4 mm thickness), and a designed structure for impact. The impact structure ensures a relatively large contact surface area between the piezo stack transducer system and the inertial mass system when the collision occurs. Two plate springs are placed on the top and bottom of the inertial mass respectively to adjust the desired low resonant frequencies and guide the motion of the inertial mass. The piezo stack system comprises a 0.15 kg cylindrical added mass, two plate springs made of spring steel (0.3 mm thickness with the stiffness  $K_1 = 964$  N/m) and a piezo stack transducer. The piezo stack transducer is assembled

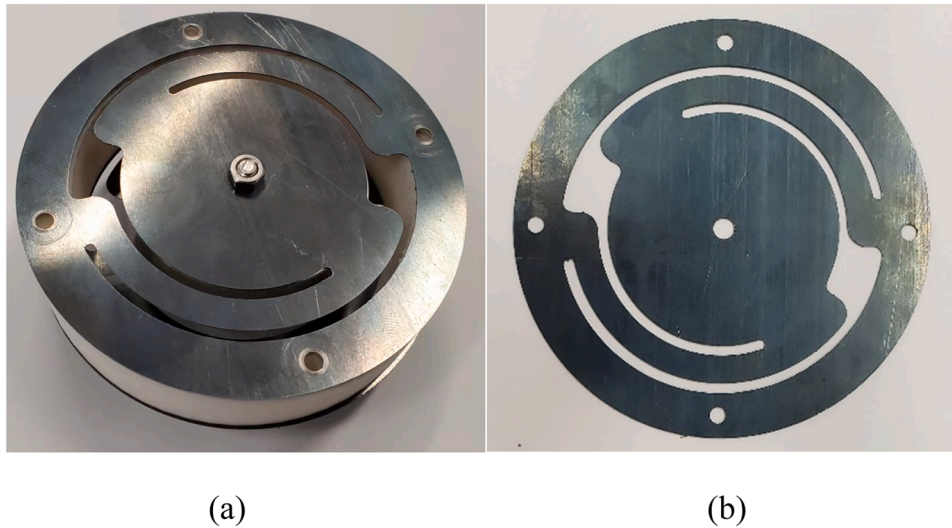


Fig. 9. The designed (a) inertial mass system and (b) plate springs for the inertial mass system.

using a 560-layer piezo stack operating in 33-mode ( $7 \times 7 \times 36$  mm, Thorlabs) and a mechanical transformer made of spring steel. These two systems are assembled into one compact design through four screws as shown in Fig. 10(a). The dimensions and material properties of the developed energy harvester are summarised in Table 1.

#### 4.2. Experimental setup

The experimental setup for the energy harvester is shown in Fig. 10 (b). The prototype is installed on an electromagnetic shaker (APS 113), which is driven by the signal derived from a signal generator (Tektronix AFG3022C) and then amplified by a power amplifier (APS 125). The acceleration generated by the shaker is measured by an accelerometer (Kistler 8762A5). The energy harvester is connected to a variable load resistor. The voltage across the load resistor and the measured signal from the accelerometer are measured using a NI cDAQ-9174 and recorded through LabVIEW software. This voltage is then used to calculate the power generated by the harvester.

### 5. Results and discussions

#### 5.1. Experimental validation of power generation simulation

##### 5.1.1. Time domain responses

Fig. 11 shows the measured and simulated time-domain responses of voltage and power output with a load resistor of  $200 \Omega$  at the excitation

Table 1

Dimensions and material properties of the developed energy harvester.

|               | Description  | Value                    |
|---------------|--|--------------------------|
| Piezo stack   | Density ( $\text{kg}/\text{m}^3$ )                       | 7700                     |
|               | Piezoelectric charge constant $d_{33}$ ( $10^{-12}$ C/N) | 710                      |
|               | Coupling factor $K_{33}$                                 | 0.63                     |
|               | Mechanical transformer                                   |                          |
|               | Material   | Spring steel (60Si2CrVA) |
|               | Density ( $\text{kg}/\text{m}^3$ )                       | 7850                     |
|               | Young's modulus (GPa)                                    | 207                      |
|               | Poisson's ratio  | 0.3                      |
|               | Dimension (mm)   | $46 \times 27 \times 7$  |
|               | Tilted angle   | $6^\circ$                |
| Inertial mass | Mass (kg)  | 0.3                      |
| Added mass    | Mass (kg)  | 0.15                     |

of 17 Hz and 0.7 RMS g. The initial interval  $d_0$  is set to be 0.1 mm. The energy harvester has two types of behaviour during each cycle, as described in Section 2, which can be observed in the voltage and power responses. When the inertial mass system collides with the piezo stack system, the voltage changes from 0 to maximum in a short period while the power reaches maximum accordingly. When the inertial mass detaches, the piezo stack system vibrates freely at its resonance frequency (94 Hz), and thus the voltage and power decays gradually under the free vibration. In this way, the proposed energy harvester transforms the excitation of 17 Hz into the piezo stack transducer's high resonant

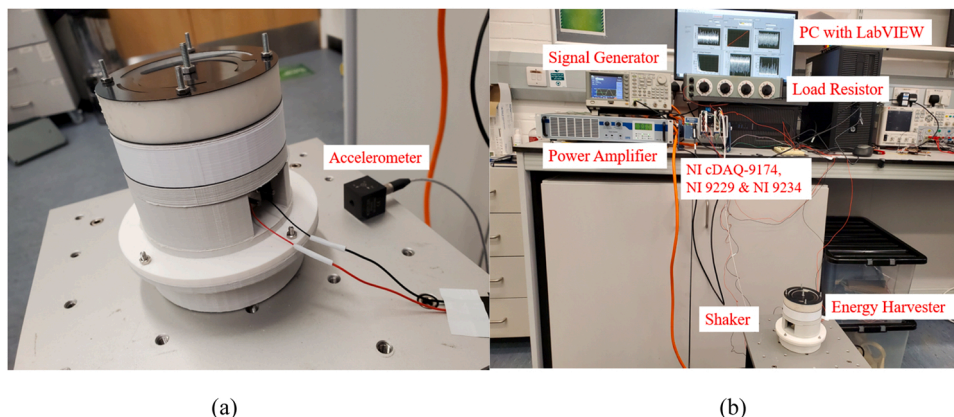


Fig. 10. (a) The compact energy harvester mounted onto a shaker, and (b) experimental setup for the energy harvester.

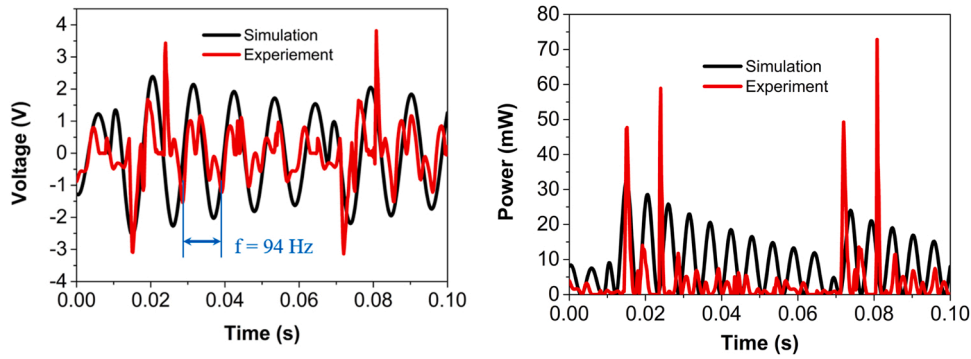


Fig. 11. The measured and simulated time-domain responses of voltage and power output with a load resistor of 200 Ω at the excitation of 17 Hz and 0.7 RMS g.

frequency vibration of 94 Hz, realising the goal of frequency up-conversion. It is noted that there are two peaks in each oscillation of the system for the experiment, while there is only one peak for the simulation. This is because the plate springs on the added mass of the piezo stack system in the experiment transform some of the oscillation motion into a slight torsion. In general, the simulated and experimental results are consistent with each other.

5.1.2. Frequency domain responses

After understanding the time-domain responses, we need to evaluate the frequency responses. Fig. 12(a) shows the measured and simulated frequency responses of the average power of the energy harvester with a load resistor of 200 Ω at the RMS acceleration of 0.7 g. In the experiment, when the excitation frequency is away from the natural frequencies of the inertial mass system (below 6 Hz and above 23 Hz), the average power is rather low and below 1 mW. When the excitation frequency is near the natural frequencies (7–16 and 21–22 Hz), the mass system can slightly collide with the piezo stack system, and thus the output voltage and power are improved on a small scale. When the excitation frequency equals the natural frequencies (17–20 Hz), the mass system exerts a large impact force on the piezo stack system, and the output voltage and power are significantly improved. Experimental results show that the amplitude voltage reaches 4.01 V and the RMS voltage is 1.16 V, while the maximum power reaches 114.5 mW and the average power is 6.72 mW actuated at 20 Hz. It is noticed that the frequency responses have two peaks (17 Hz and 20 Hz for both experiment and simulation). The experiment results show a higher output near the natural frequencies (6–14 Hz) compared to simulation results, which

may be caused by the nonlinearity of the plate springs and collision motion. In general, the frequency responses of the simulation and experiment validate the unique characteristic of the proposed system. The system has two modes of vibration due to the plate springs on the inertial mass and the mode shape is shown in Fig. 12(b). The first mode of vibration (17 Hz), also called longitudinal mode, is caused by the oscillation of the plate springs along the vibration direction. The second mode of vibration (20 Hz), also called torsional mode, is due to the torsion of the plate springs. This characteristic is beneficial to broadening the frequency bandwidth of the energy harvester.

5.2. 5.2 Experimental evaluation of factors affecting power generation

5.2.1. Load resistance

Fig. 13 shows the amplitude voltage, RMS voltage, maximum power and average power of the energy harvester actuated at 17 Hz and 0.7 RMS g across a range of load resistance. The highest average and maximum power occur at a load resistance of 200 Ω. As a result, an optimal load resistance of 200 Ω is determined, which is used for further tests.

5.2.2. Input acceleration

Fig. 14 depicts the frequency responses of average power with different input RMS accelerations of 0.5 g, 0.6 g, and 0.7 g. In general, the power output increases with the acceleration and the overall trends of the frequency responses with different accelerations are the same. It is because as the acceleration increases, the inertial mass system has larger displacements and collides with the piezo stack transducer system with a

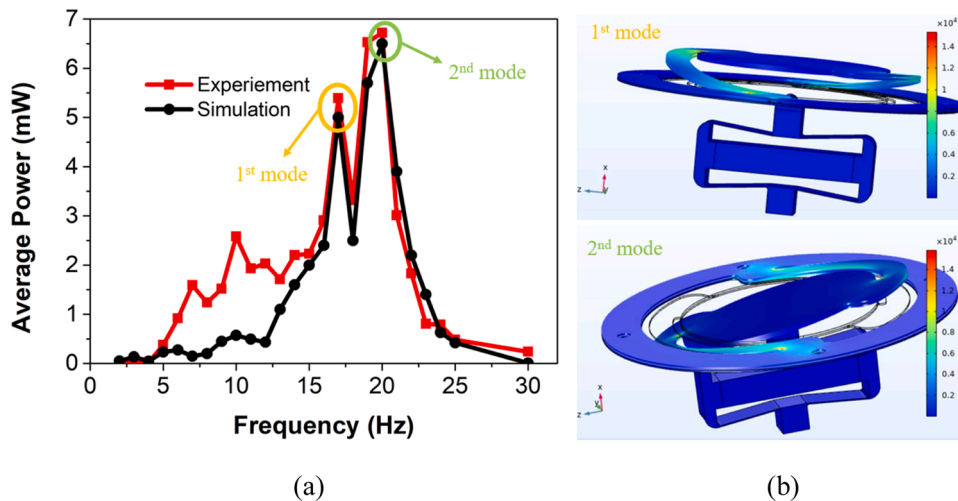


Fig. 12. (a) The measured and simulated frequency responses of the average power of the energy harvester with a load resistor of 200 Ω at the RMS acceleration of 0.7 g, and (b) Mode shape of the energy harvester.

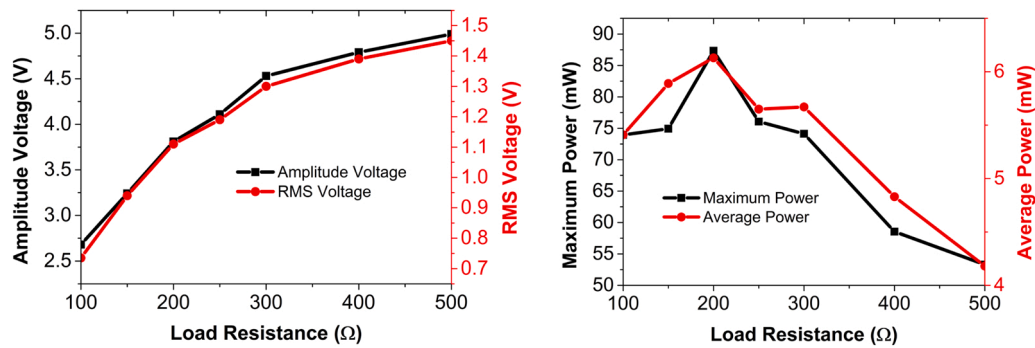


Fig. 13. The voltage amplitude voltage, RMS voltage, maximum power and average power of the energy harvester actuated at 17 Hz and 0.7 RMS g across a range of load resistance.

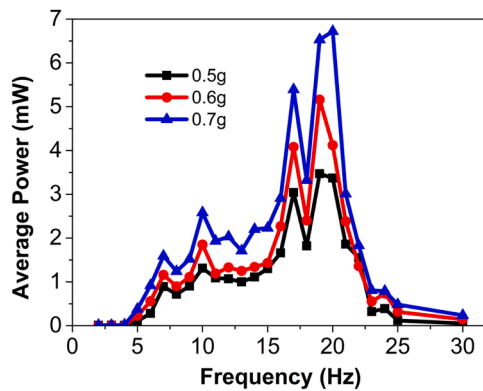


Fig. 14. The frequency responses of average power with different RMS accelerations of 0.5 g, 0.6 g, and 0.7 g.

larger impact force, resulting in higher power output. It is noted that the average power is approximately proportional to the squared acceleration. Meanwhile, the energy harvester with different accelerations has the same initial relative position and arrangement between the inertial mass and piezo stack systems. As a result, the stiffness of the system does not change, and thus the resonant frequencies remain the same.

### 5.2.3. Initial interval

Fig. 15 shows the frequency responses of average power with different initial intervals of  $-0.9$  mm,  $0.1$  mm, and  $1.1$  mm actuated at  $0.7$  RMS g. The initial intervals are adjusted by adding a  $1$  mm washer to the piezo stack transducer or inertial mass systems. The harvester with a negative initial interval means that the piezo stack system contacts with the impact structure and deforms the plate springs of the inertial mass

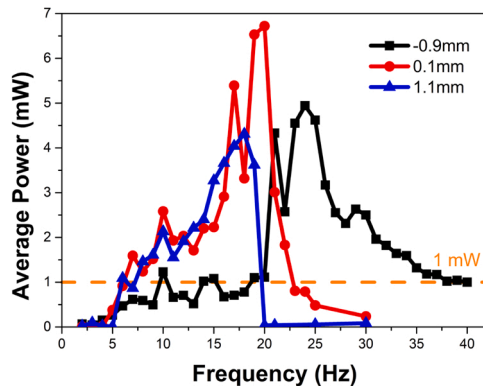


Fig. 15. The frequency responses of average power with different initial intervals of  $-0.9$  mm,  $0.1$  mm, and  $1.1$  mm actuated at  $0.7$  RMS g.

system in a static state. It is found that the initial interval greatly influences the resonant frequencies and frequency bandwidths of the harvester. The energy harvester with a  $-0.9$  mm initial interval has resonant frequencies of  $21$  Hz and  $24$  Hz achieving maximum average power of  $4.94$  mW with a  $1$ -mW-bandwidth of  $20$  Hz from  $19$  Hz to  $39$  Hz. As the initial interval increases, the resonant frequencies of the harvester shift toward lower values and the average power at resonant frequencies increases at the cost of reduced bandwidth. The resonant frequencies of the energy harvester with a  $0.1$  mm initial interval shift to  $17$  Hz and  $20$  Hz, and the maximum average power increases to  $6.72$  mW. The  $1$ -mW-bandwidth is reduced to  $15$  Hz from  $7$  Hz to  $22$  Hz. The reason is that a greater interval enables the inertial mass to have a larger displacement during vibration leading to a higher impact force at the resonant frequencies and a failure to collide at other frequencies. In other words, the two systems with lower initial intervals are easy to collide with each other, and thus the frequency bandwidth is quite broad. However, when the initial interval continues increasing, there is only one resonant frequency with reduced maximum average power and bandwidth. This is because the displacement caused by the torsional mode is lower than the initial interval, while the displacement caused by the longitudinal mode is higher than the initial interval. As a result, the collision motion can only be triggered by the first mode of vibration, and the second mode of vibration cannot be activated. The energy harvester with a  $1.1$  mm initial interval has a resonant frequency of  $18$  Hz achieving maximum average power of  $4.31$  mW with a  $1$ -mW-bandwidth of  $13$  Hz from  $6$  Hz to  $19$  Hz. If the initial interval further increases, the inertial mass system cannot collide with the piezo stack transducer system, and the frequency up-conversion mechanism cannot be realised. In general, the energy harvester with around  $0.1$  mm initial interval is desired for realising the full potential of the unique two-peak frequency response characteristic. The initial interval can be optimised by adjusting the thickness of the washer.

### 5.2.4. Plate spring

Fig. 16(a) shows the frequency responses of average power with two different stiffnesses of plate springs ( $K_2 = 2920$  N/m and  $K_3 = 44000$  N/m) on the added mass of the piezo stack transducer system actuated at  $0.7$  RMS g. The stiffness is adjusted by changing the shape of the plate springs (shown in Fig. 9 and Fig. 16(b)) with a thickness of  $0.5$  mm. As the stiffness of the plate spring becomes higher, the motion of the mechanical transformer is constrained, and thus the average power decreases and the stress of the mechanical transformer is reduced. The average power generated by the energy harvester with plate springs of  $K_3 = 44000$  N/m is remarkably low compared to that of  $K_2 = 2920$  N/m. Generally, a softer spring which can limit the torsion of the mechanical transformer is desired. The plate spring can be optimised by designing its shape and thickness.



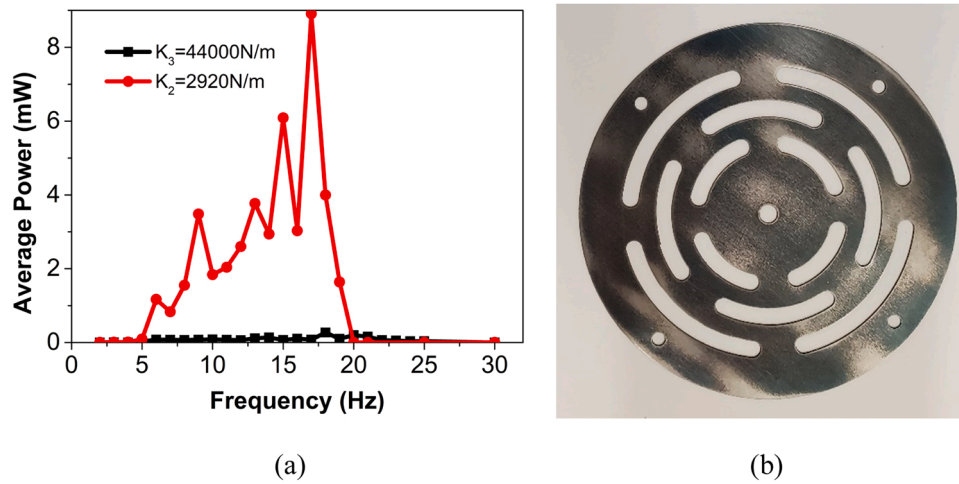


**Fig. 16.** (a) The frequency responses of average power with two different stiffnesses of plate springs ( $K_2 = 2920 \text{ N/m}$  and  $K_3 = 44000 \text{ N/m}$ ) on the added mass of the piezo stack transducer system actuated at 0.7 RMS g, and (b) the shape of the plate spring with the stiffness  $K_3 = 44000 \text{ N/m}$ .

### 5.2.5. Pulse excitation

It is reported that the track vibration excitation of the field test is more like an impulse [27], so a pulse excitation of 20 Hz and RMS acceleration of 0.7 g with a width of 20% is used as the excitation signal further to evaluate the energy harvesting performance. The time-dependent voltage and power are presented in Fig. 17. The results show that the amplitude voltage reaches 3.92 V and the RMS voltage is 0.94 V, while the maximum power reaches 121.45 mW and the average power is 4.41 mW. The time-dependent responses indicate that the frequency up-conversion mechanism can also be achieved subjected to pulse excitation. However, the average power of pulse excitation is lower than that of harmonic excitation.

### 5.3. Comparison of state-of-the-art piezoelectric energy harvesters for railway track vibration

Table 2 shows the comparison of state-of-the-art piezoelectric energy harvesters reported in the literature for rail track vibration. The proposed vibration energy harvester is found to exhibit good performance with regard to power output.

## 6. Conclusions

In this paper, a compact piezo stack energy harvester with frequency up-conversion mechanism is designed, modelled, fabricated, and tested for scavenging energy from railway track vibration. Several designs are carried out to meet railway track applications requirements in size, frequency, and stress. A compact design integrating the inertial mass and the piezo stack transducer systems is used to enable the mechanical

collision for realising the frequency up-conversion mechanism and ensure the size of the energy harvester is suitable for the limited space on the railway track. The frequency bandwidth of the energy harvester is broadened by using the two adjacent natural frequencies design, which is implemented through the two modes of vibration of the inertial mass system. The first vibration mode is caused by the oscillation of the plate springs along the vibration direction, while the second vibration mode is due to the torsion of the plate springs. The mechanical transformer of the piezo stack transducer system, which is the weakest part of the energy harvester, is designed to achieve the required stress level under both the impact force caused by the collision motion and the inertial force generated by the random vibration of the rails. A FEM model is developed to analyse the free vibration of the piezo stack transducer specifically generated by the impact between the inertial mass system and the piezo stack transducer system. The proposed FEM model first computes the displacements of the piezo stack transducer system under the impact, which is then used as initial displacements for the time-dependent power output simulation. Comparisons between simulation and experiment validate the two adjacent modes of vibration responses of the system.

Lab tests are further conducted to evaluate the impact of different factors such as load resistance, input acceleration, initial interval, plate spring, and pulse excitation on power generation. The experimental results show that the harvester effectively converts a low-frequency vibration into the piezo stack transducer's high resonant frequency vibration from 17 Hz to 94 Hz. A maximum average power of 6.72 mW with a 1-mW-bandwidth of 15 Hz is obtained when actuated at 0.7 RMS g acceleration. It is noted that the average power is approximately proportional to the squared acceleration. Moreover, the initial interval

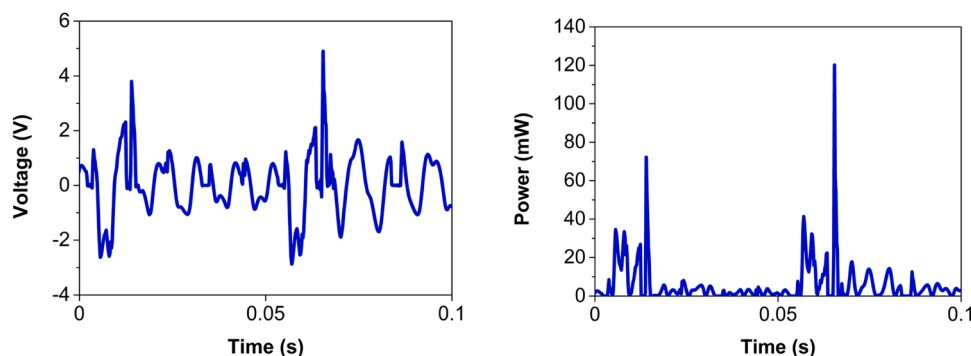


**Fig. 17.** The time-dependent voltage and power with a load resistor of 200  $\Omega$  at a pulse excitation of 20 Hz and 0.7 RMS g.

**Table 2**  
Comparison of state-of-the-art piezoelectric energy harvesters for railway track vibration.

| References         | Harvester volume [mm <sup>3</sup> ]            | Proof mass [g] | Resonant frequency [Hz] | Test       | Acceleration [g]          | Load impedance [kΩ] | Power [mW]                 |
|--------------------|--|----------------|-------------------------|------------|---------------------------|---------------------|----------------------------|
| Nelson et al. [28] |  |                |                         | Field      |                           | 387                 | 0.053 (ave)                |
| Li et al. [27]     | (30–35) × 10 × 0.5                             | 3.48–4.08      | 55–75                   | Lab        | 0.2                       | 59.4                | 0.2 (ave)                  |
| Wang et al. [29]   | 20 × 20 × 0.2 (patch)<br>50 × 50 × 165 (stack) |                |                         | Simulation | Train speed of 30 m/s     | 211                 | 0.19 (rms)                 |
| Mishra et al. [30] | 36 × 0.6 × 0.16                                | 5              | 93.54                   | Simulation | Train speed of 30 m/s     | 180                 | 0.027 (rms)                |
| Gao et al. [11]    | 200 × 170 × 80                                 | 60             | 7                       | Lab        | 5                         | 100                 | 4.88 (peak)                |
| Yang et al. [31]   | 38.1 × 200 × 15.6                              | 2.58           | 61.7 & 691.0            | Simulation | 2.91 m/s <sup>2</sup> /Hz | 55.24               | 1 mW/Hz (peak)             |
| Cao et al. [14]    | Ø113 × 148                                     |                | 5                       | Lab        | Displacement of 2 mm      | 12                  | 0.34 (ave)                 |
| This work          | Ø90 × 82                                       | 300 + 150      | 17 & 20                 | Lab        | 0.7 (rms)                 | 0.2                 | 6.72 (ave)<br>114.5 (peak) |

greatly influences the resonant frequencies and frequency bandwidth of the harvester. As the initial interval increases, the average power at resonant frequencies increases at the cost of reduced bandwidth. However, when the initial interval is larger than the displacement caused by the torsional mode and lower than the displacement caused by the longitudinal mode, the resonant frequencies change from two to one, and the second mode of vibration cannot be activated. Furthermore, a harder spring on the piezo stack transducer system reduces the stress of the mechanical transformer while resulting in lower power output. Therefore, a softer spring which can limit the torsion of the mechanical transformer is needed in the piezo stack transducer system.

#### CRedit authorship contribution statement

All authors have seen and approved the final version of the manuscript being submitted. The article is the authors' original work, hasn't received prior publication and isn't under consideration for publication elsewhere, Guansong Shan, Dr. Yang Kuang, Prof. Meiling Zhu.

#### Declaration of Competing Interest

The authors declare that they have no known competing financial interests or personal relationships that could have appeared to influence the work reported in this paper.

#### Data Availability

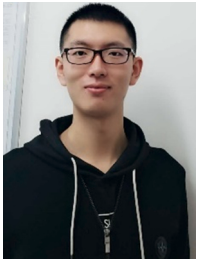
Data will be made available on request.

#### Acknowledgement

The authors would like to acknowledge the support of the EPSRC through the Project Zero Power, Large Area Rail Track Monitoring under Grant EP/S024840/1 and also the support of University of Exeter.

#### References

- [1] UIC, Railway statistics — synopsis year 2021, International Union of Railways (UIC), Paris.
- [2] G.R. PENAMALLI, Structural health monitoring and energy harvesting for railroad, *Mech. Eng., Stony Brook Univ.* (2011) 111.
- [3] M. Gao, P. Wang, Y. Cao, R. Chen, D. Cai, Design and verification of a rail-borne energy harvester for powering wireless sensor networks in the railway industry, *IEEE Trans. Intell. Transp. Syst.* (2016) 1–14.
- [4] Y. Pan, T. Lin, F. Qian, C. Liu, J. Yu, J. Zuo, L. Zuo, Modeling and field-test of a compact electromagnetic energy harvester for railroad transportation, *Appl. Energy* 247 (2019) 309–321.
- [5] S. Bradai, S. Naifar, C. Viehweger, O. Kanoun, Electromagnetic vibration energy harvesting for railway applications, *MATEC Web Conf.* 148 (2018).
- [6] N. Bosso, M. Magelli, N. Zampieri, Application of low-power energy harvesting solutions in the railway field: a review, *Veh. Syst. Dyn.* (2020) 1–31.
- [7] Y. Pan, L. Zuo, M. Ahmadian, A half-wave electromagnetic energy-harvesting tie towards safe and intelligent rail transportation, *Appl. Energy* 313 (2022), 118844.
- [8] C. Covaci, A. Gontean, Piezoelectric energy harvesting solutions: a review, *Sensors* 20 (2020).
- [9] E. MaghsoudiNia, N.A. WanAbdullahZawawi, B.S. MahinderSingh, Design of a pavement using piezoelectric materials, *Mater. und Werkst.* 50 (2019) 320–328.
- [10] L. Wu, X.-D. Do, S.-G. Lee, D.S. Ha, A self-powered and optimal sshi circuit integrated with an active rectifier for piezoelectric energy harvesting, *IEEE Trans. Circuits Syst. I Regul. Pap.* 64 (2017) 537–549.
- [11] M.Y. Gao, P. Wang, Y. Cao, R. Chen, C. Liu, A rail-borne piezoelectric transducer for energy harvesting of railway vibration, *J. Vibroengineering* 18 (2016) 4647–4663.
- [12] M. Wischke, M. Masur, M. Kröner, P. Woias, Vibration harvesting in traffic tunnels to power wireless sensor nodes, *Smart Mater. Struct.* 20 (2011).
- [13] H. Fu, W. Song, Y. Qin, E.M. Yeatman, Broadband vibration energy harvesting from underground trains for self-powered condition monitoring, *Power* 2019, Krakow Pol. (2019) 5.
- [14] Y. Cao, R. Zong, J. Wang, H. Xiang, L. Tang, Design and performance evaluation of piezoelectric tube stack energy harvesters in railway systems, *J. Intell. Mater. Syst. Struct.* (2022), 1045389×221085654.
- [15] G. Shan, M. Zhu, A piezo stack energy harvester with frequency up-conversion for rail track vibration, *Mech. Syst. Signal Process.* 178 (2022), 109268.
- [16] W. Zhai, K. Wang, C. Cai, Fundamentals of vehicle–track coupled dynamics, *Veh. Syst. Dyn.* 47 (2009) 1349–1376.
- [17] H. Jiang, L. Gao, Study of the vibration-energy properties of the CRTS-III track based on the power flow method, *Symmetry* 12 (2020).
- [18] D.M.T.P. Division, MOD UK railways permanent way design and maintenance: policy and standards, M. o. Def. (2009).
- [19] X. Sheng, C.J.C. Jones, D.J. Thompson, A comparison of a theoretical model for quasi-statically and dynamically induced environmental vibration from trains with measurements, *J. Sound Vib.* 267 (2003) 621–635.
- [20] V.G. Cleante, M.J. Brennan, G. Gatti, D.J. Thompson, On the target frequency for harvesting energy from track vibrations due to passing trains, *Mech. Syst. Signal Process.* 114 (2019) 212–223.
- [21] F. Qian, S. Zhou, L. Zuo, Improving the off-resonance energy harvesting performance using dynamic magnetic preloading, *Acta Mech. Sin.* 36 (2020) 624–634.
- [22] H. Zhao, W. Hui, Y. Nie, Y. Weng, H. Dong, Very high cycle fatigue fracture behavior of high strength spring steel 60Si2CrVA, *Chin. J. Mater. Res* 22 (2008) 526–532.
- [23] N.A. Siddiqui, S. Ahmad, Dynamic behaviour of tension leg platform under impulsive loading, *Def. Sci. J.* 53 (2003) 205.
- [24] D.-X. Cao, X.-J. Duan, X.-Y. Guo, S.-K. Lai, Design and performance enhancement of a force-amplified piezoelectric stack energy harvester under pressure fluctuations in hydraulic pipeline systems, *Sens. Actuators A Phys.* 309 (2020), 112031.
- [25] L. Wang, S. Chen, W. Zhou, T.-B. Xu, L. Zuo, Piezoelectric vibration energy harvester with two-stage force amplification, *J. Intell. Mater. Syst. Struct.* 28 (2017) 1175–1187.
- [26] Y. Kuang, Z.J. Chew, M. Zhu, Strongly coupled piezoelectric energy harvesters: Finite element modelling and experimental validation, *Energy Convers. Manag.* 213 (2020).
- [27] J.P. Lynch, K.-W. Wang, H. Sohn, J. Li, S. Jang, J. Tang, Implementation of a piezoelectric energy harvester in railway health monitoring, *Sensors and Smart Structures Technologies for Civil, Mech., Aerosp. Syst.* 2014 (2014).
- [28] C.A. Nelson, S.R. Platt, D. Albrecht, V. Kamarajugadda, M. Fateh, Power harvesting for railroad track health monitoring using piezoelectric and inductive devices, *Act. Passiv. Smart Struct. Integr. Syst.* 2008 (2008).
- [29] J. Wang, Z. Shi, H. Xiang, G. Song, Modeling on energy harvesting from a railway system using piezoelectric transducers, *Smart Mater. Struct.* 24 (2015).
- [30] M. Mishra, P. Mahajan, R. Garg, Piezoelectric Energy Harvesting System Using Railway Tracks. *Innovations in Electrical and Electronic Engineering*, Springer, 2021, pp. 247–259.
- [31] F. Yang, M. Gao, P. Wang, J. Zuo, J. Dai, J. Cong, Efficient piezoelectric harvester for random broadband vibration of rail, *Energy* 218 (2021).



**Guansong Shan** received the B.Eng. and M.Eng. degrees in mechanical engineering from Jilin University, Changchun, China. He is currently working towards his PhD in Energy Harvesting at the University of Exeter, Exeter, U.K. His current research focuses on piezoelectric energy harvesters for railway track vibration.



**Yang Kuang** received the B.Eng. and M.Eng. degrees in mechanical engineering from Central South University, Changsha, China, and the Ph.D. degree in high power piezoelectric transducers from the University of Dundee, Dundee, Scotland, in 2014. Since 2014, he has been with the University of Exeter, as an Associate Research Fellow and later as a Research Fellow. His main research interest includes self-power wireless sensing systems enabled by energy harvesting.



**Meiling Zhu** received the B.Eng. degree in mechanical manufacturing, the M.Eng. degree in applied mechanics, and the Ph.D. degree in mechanical dynamics all from Southeast University, Nanjing, China, in 1989, 1992, and 1994, respectively. She currently holds the Professor and the Chair in Mechanical Engineering and the Head of Energy Harvesting Research Group in the University of Exeter, Exeter, U.K. Prior to joining the University of Exeter, she was with a number of Universities: Cranfield University (2002–2013), the University of Leeds (2001–2002); Stuttgart Universität (1999–2001); the Hong Kong University of Science and Technology (1998–1999); and the Institute of Vibration Engineering Research in the Nanjing University of Aeronautics and Astronautics (1994–1998). Her current research interest includes the area of piezoelectric energy harvesting powered wireless sensor nodes for applications.